Sixteen years of SABER measurements and the MSIS model were used to study the intra-annual SAO and AO of kzz (eddy diffusion) in the mesosphere (80-96 km).

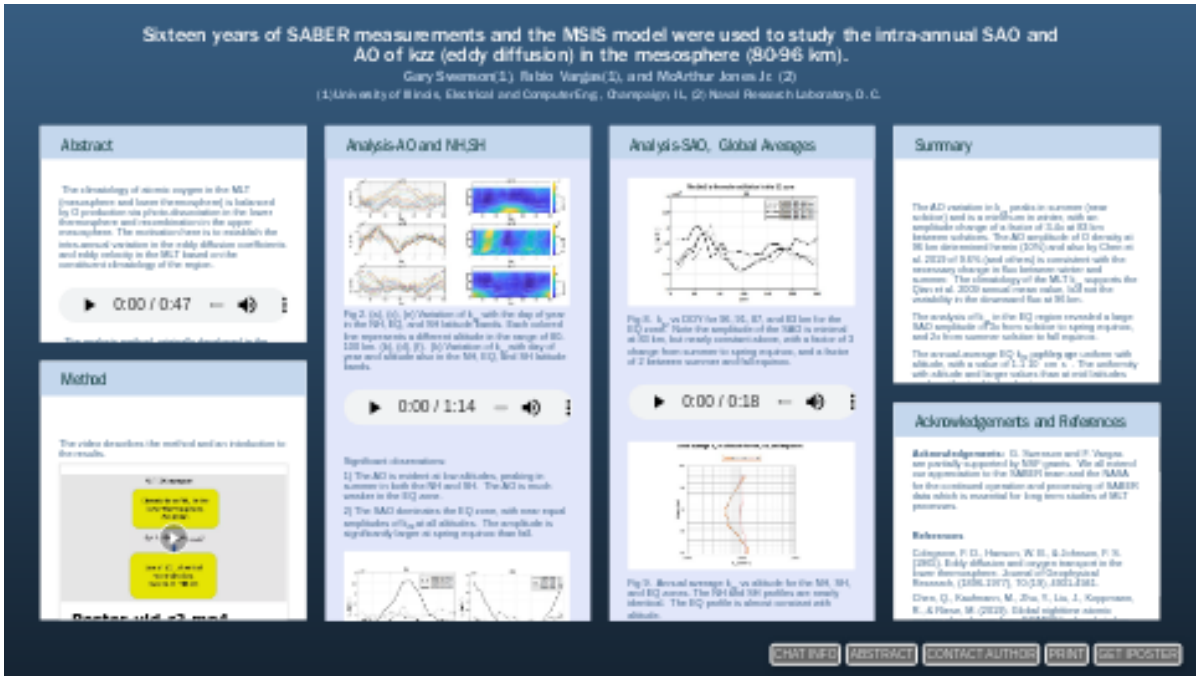

Gary Swenson(1), Fabio Vargas(1), and McArthur Jones Jr. (2)

(1) University of Illinois, Electrical and Computer Eng., Champaign, IL, (2) Naval Research Laboratory, D. C.

PRESENTED AT:

AGU FALL MEETING
Online Everywhere | 1–17 December 2020

ABSTRACT

The climatology of atomic oxygen in the MLT (mesosphere and lower thermosphere) is balanced by O production via photo-dissociation in the lower thermosphere and recombination in the upper mesosphere. The motivation here is to establish the intra-annual variation in the eddy diffusion coefficients and eddy velocity in the MLT based on the constituent climatology of the region.

The analysis method, originally developed in the 60's (Colegrove et al. 1965), was refined for a study of the MLT global inter-annual variations and global mean values (see Swenson et al. 2018, 2019, respectively). In the this study, the intra-annual cycle was divided into twenty-six (two-week) periods for each of three zones, the northern hemisphere (NH, 15 to 55^o), southern hemisphere (SH, -15 to -55^o), and the equatorial region (EQ, 15 to -15^o). Sixteen years of SABER O density measurements (2002-2018) and NRLMSIS 2.0 (Emmert et al., 2020) N_2 , O_2 and T profiles (80-96 km) were used for each of the periods and zones for the determination of O eddy diffusion velocities and fluxes.

Atomic oxygen diffusive fluxes ($[O].v_{eddy}$, 80-96 km) are balanced by the continuity of chemical loss, but the intra-annual variation of k_{zz} (determined from veddy) and [O] are determined separately.

The major findings include:

1) A dominant AO below 87 km in the NH and SH zones, with the largest variation in amplitude between winter and summer at 83 km.

2) A dominant SAO at all altitudes (80-96 km) in the EQ zone.

3) Intra-annual variability in the global average [O] and k_{zz} contribute to variability of O eddy transport in the MLT.

METHOD

The video describes the method and an intoduction to the results.

Atomic oxygen (O) is produced via photodissociation above 110 km, and lost, primarily through chemical recombination, with a maximum loss near 88 km.

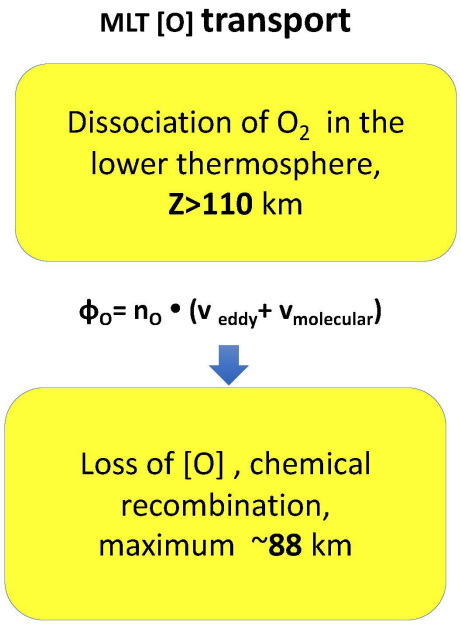

Fig 1. MLT O transport schematic.

The primary transport mechanism for O is diffusion, where the total diffusive flux (nv), and velocity is the sum of the molecular and eddy components (eqn 1, S19).

The integral loss rate of O, via chemistry, is assumed to be supplied by the downward diffusive flux (eqn 2). Note in the presentation eddy flux is a catch-all term in this context, since [O] could include contributions from large scale waves (e.g., tides) and vertical winds.

$$\phi_O(z) = -D_i[O]\left(\frac{1}{H_i} + \frac{1}{T}\frac{dT}{dz} + \frac{1}{[O]}\frac{d[O]}{dz}\right) - k_{zz}[O]\left(\frac{1}{H} + \frac{1}{T}\frac{dT}{dz} + \frac{1}{[O]}\frac{d[O]}{dz}\right) \quad (1)$$

$$\phi_O(z) = \int_{z=80}^{z} (-2k_1[O][O_2][M] - 2k_4[O]^2[M] - 2k_6[H][O_2][M])dz' \quad (2)$$

$$v_{O,eddy}(z) = v_O(z) - v_{O,md}(z) \quad (3)$$

$$k_{zz} = -\frac{v_{O,eddy}}{\left(\frac{1}{H} + \frac{1}{T}\frac{dT}{dz} + \frac{1}{[O]}\frac{d[O]}{dz}\right)} \quad (4)$$

The year was divided into 26, 2-week periods, for 3 zones, the NH, SH, and the EQ . A consideration for the two-week minimum is the diffusion times between altitudes of production and loss (see S19). in each zone, for each period, 16-year average SABER O (Mlynczak et al. 2013) density profiles were used, and N_2, O_2, and T values were determined from NRLMSIS 2.0 model (Emmert et al. 2020), where 40^o latitude was used for the NH and SH, and 0^o for the EQ. The eddy velocity is determined by subtracting the molecular component (eqn 3), and subsequently, k_{zz} values were determined (eqn 4).

In summary, the climatology of composition, including SABER [O], was used to determine the diffusion velocity (and k_{zz}) in each zone. The eddy diffusion velocity is strongly related to the vertical gradient in [O], and weakly on the O density. The intra-annual variation in [O] may have separate variations due to planetary waves, production vs solar elevation angle, as well as other geophysical forcing. The NRLMSIS 2.0 values for each of the temporal/spatial zones used an average $F_{10.7}$ value for the 16-year period and the seasonal variation (day of year).

ANALYSIS-AO AND NH,SH

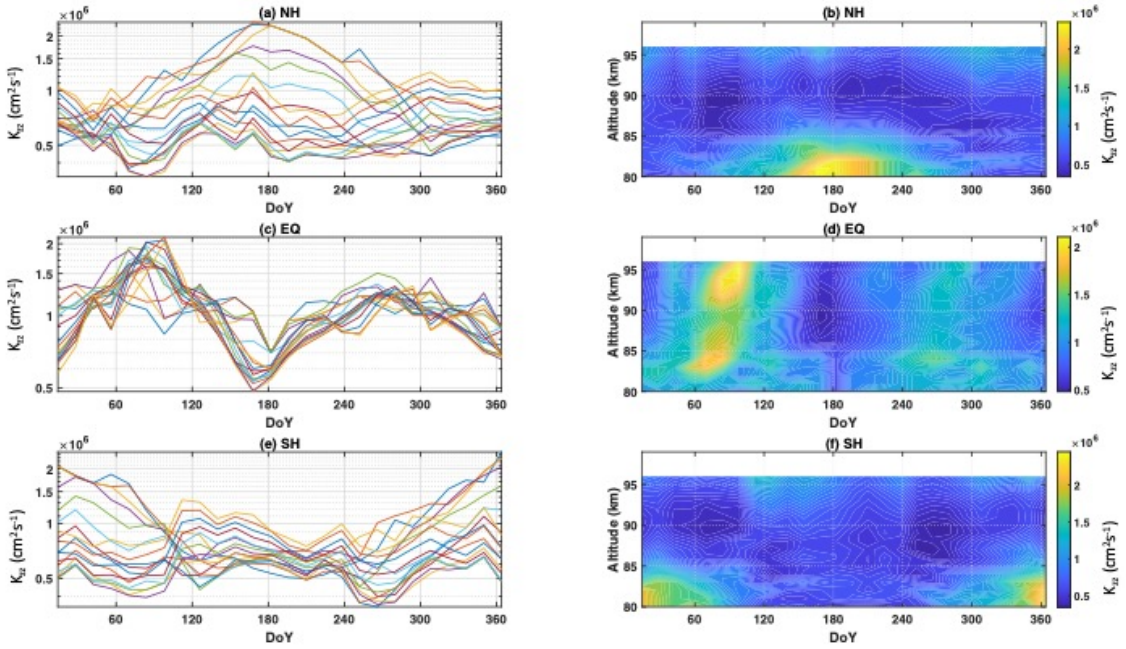

Fig 2. (a), (c), (e) Variation of k_{zz} with the day of year in the NH, EQ, and SH latitude bands. Each colored line represents a different altitude in the range of 80-100 km. (b), (d), (f). (b) Variation of k_{zz} with day of year and altitude also in the NH, EQ, and SH latitude bands.

Significant observations:

1) The AO is evident at low altitudes, peaking in summer in both the NH and SH. The AO is much weaker in the EQ zone.

2) The SAO dominates the EQ zone, with near equal amplitudes of k_{zz} at all altitudes. The amplitude is significantly larger at spring equinox than fall.

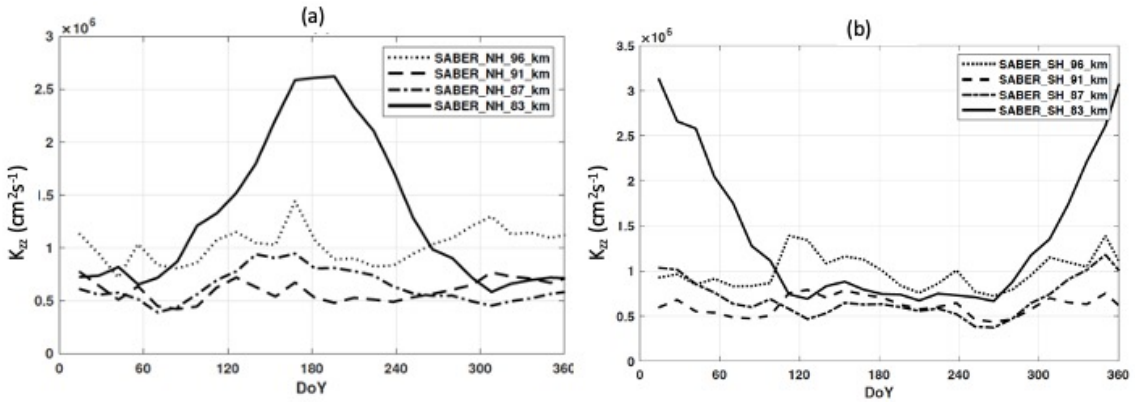

Fig 3. (a) K_{zz} vs DOY for the NH 96, 91, 87, and 83 km. The AO, has a minimum at winter solstice and a maximum at summer. (b) Same as (a) except the SH.

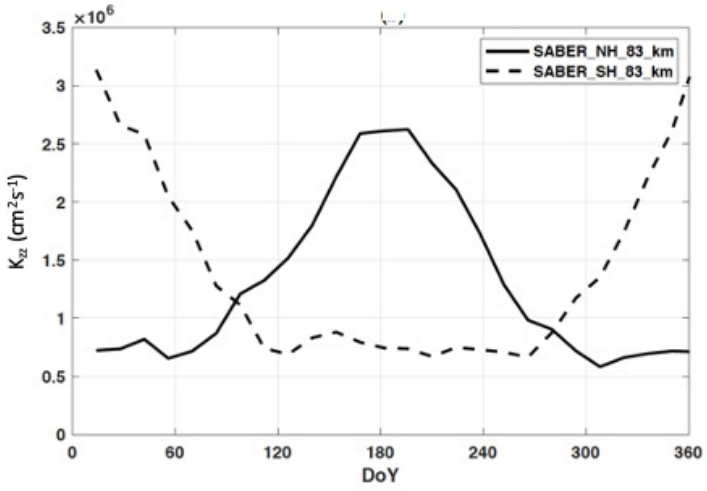

Fig 4. k_{zz} vs DOY for the NH (solid) and SH (dashed) at 83 km. The AO amplitude is a factor of 3-4x change from winter to summer.

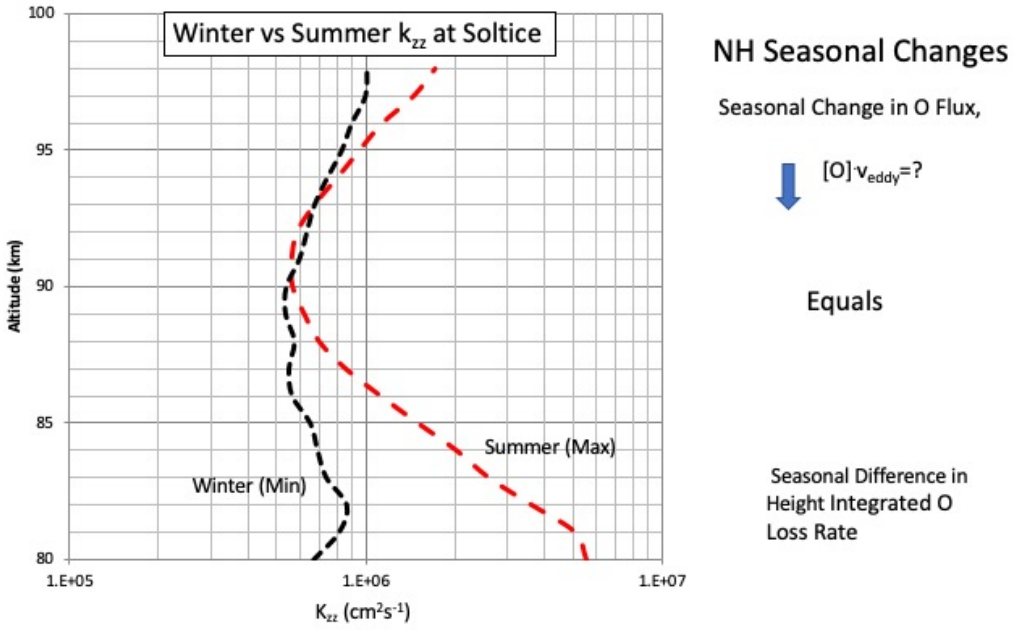

Fig 5. k_{zz} vs altitude for summer and winter soltice in the NH. The downward flux of O at 96 km should account for the change in the integral loss of O for the two k_{zz} profiles.

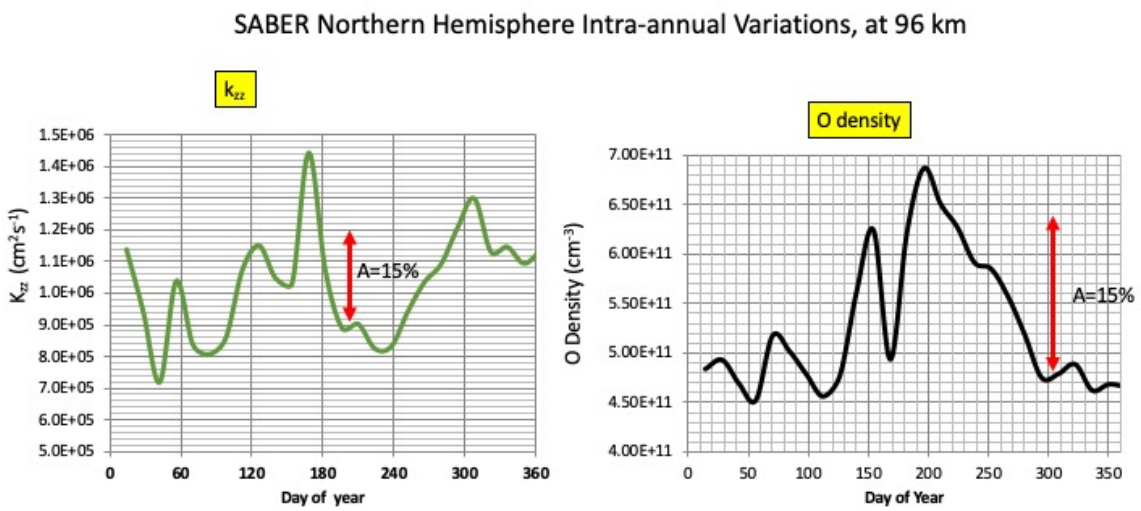

Fig 6. The intra-annual variation of k_{zz} (left) and [O] (right) are shown with vertical scale illustrating a scale of change.

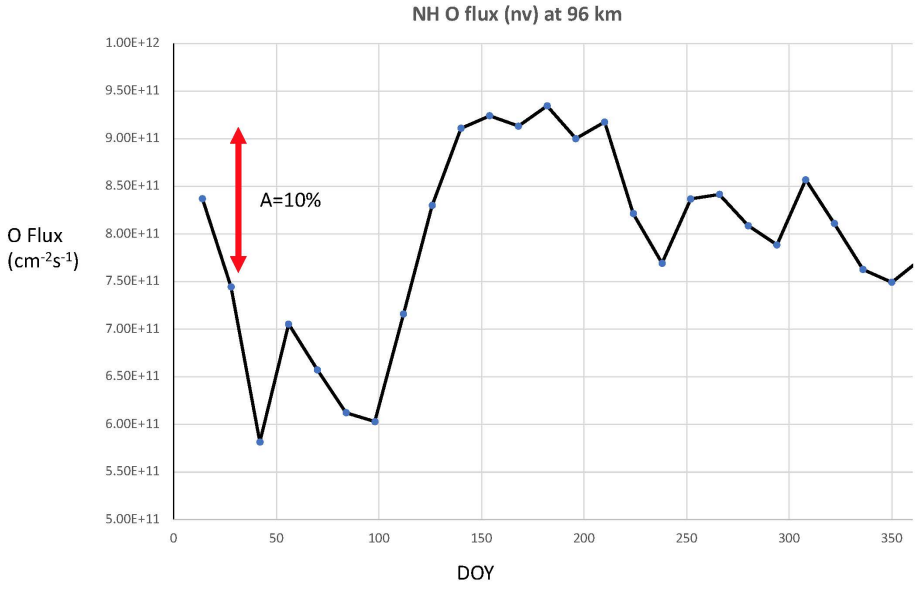

Fig 7. The intra-annual variation of the eddy flux, in the NH at 96 km has a maximum in summer, with lower values in fall, and significantly lower in spring. The vertical arrow illustrates the required change between summer and winter that is required to account for the change in the AO loss of O below 87 km.

ANALYSIS-SAO, GLOBAL AVERAGES

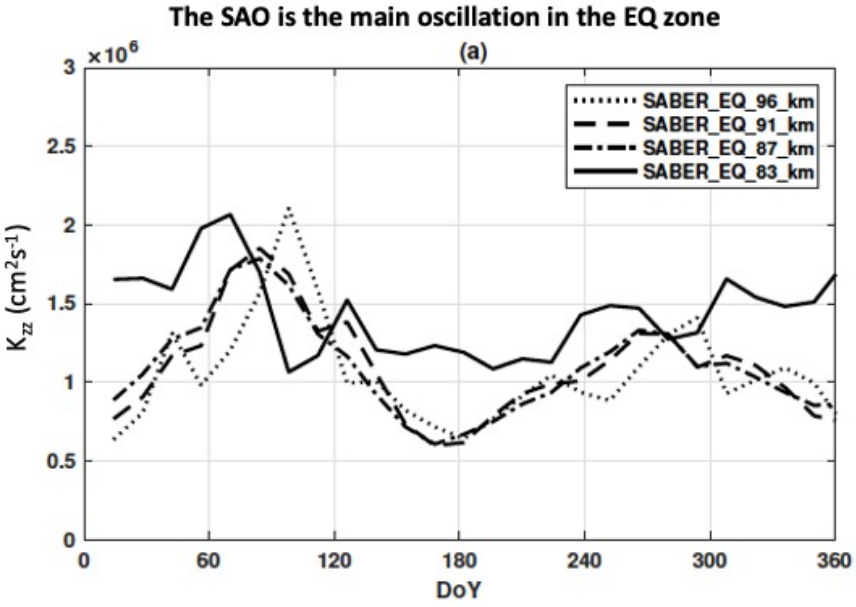

Fig 8. k_{zz} vs DOY for 96, 91, 87, and 83 km for the EQ zone. Note the amplitude of the SAO is minimal at 83 km, but nearly constant above, with a factor of 3 change from summer to spring equinox, and a factor of 2 between summer and fall equinox.

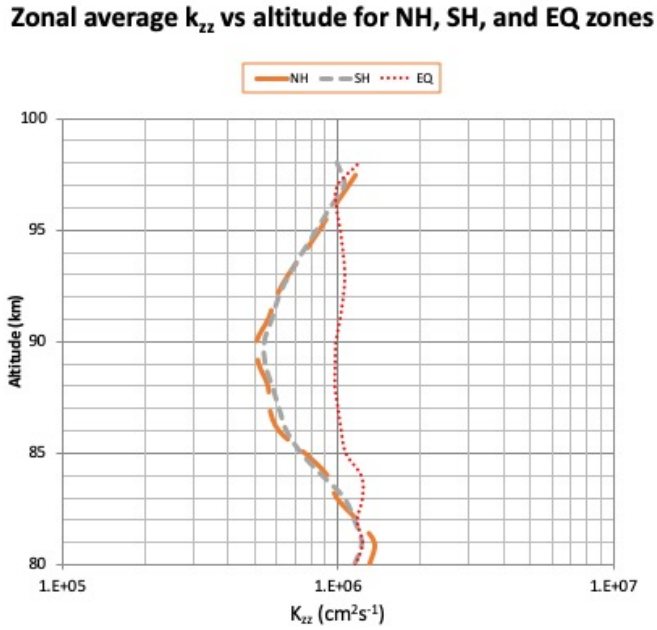

Fig 9. Annual average k_{zz} vs altitude for the NH, SH, and EQ zones. The NH and SH profiles are nearly identical. The EQ profile is almost constant with altitude.

On explanation for the larger and near constant profile in the low latitudes is 1) the likely difference in the shape of the profile with altitude is wave-tide interaction, where the low latitude presence of the diurnal tide couples with AGWs, resulting in shear and convective instabilities, and a larger k_{zz}. 2) In addition, the well understood stratospheric dynamics which filter waves from reaching the MLT region is minimal at the low latitudes, enabling waves to propagate to the MLT during all seasons.

Intra-annual Global Means

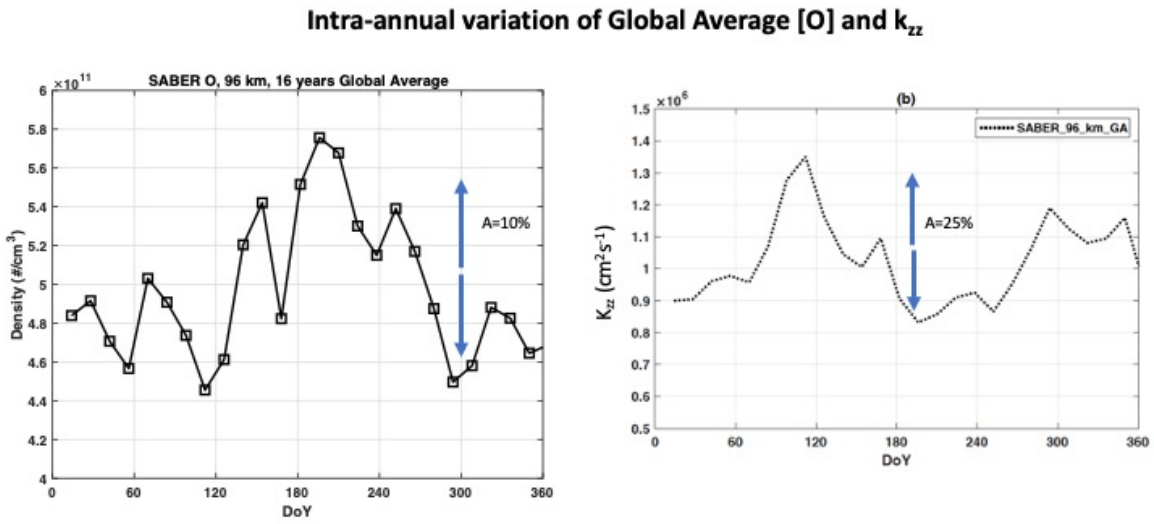

Fig 10. (a) Intra-annual variations in O density averaged between -/+ 55 deg at 96 km, describes an AO amplitude of 10%. (b) The global average kzz vs day of year for SABER at 96 km. There is a negligible difference between winter and summer, although the SAO is significant.

The measurement of a 10% amplitude of [O] density at 96 km, was also observed in OH airglow by the GOMOS instrument on Envisat with an amplitude of 9.6% from OH emission (Chen et al. 2019). Similar, analysis by Zhao et al. (2015) and Lednyts'kyy et al. (2017) determined AO amplitudes of 7% and 11%, respectively.

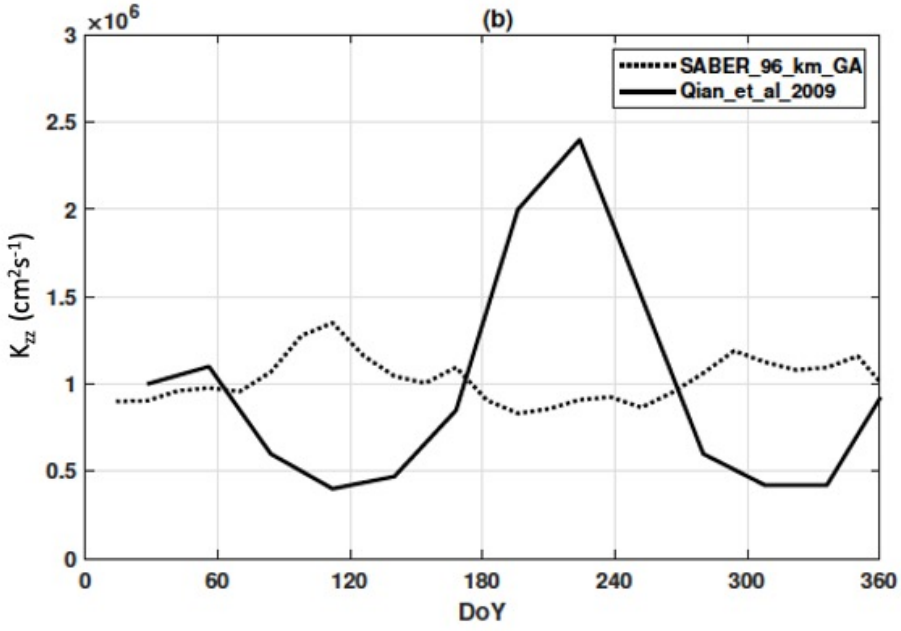

Fig 11. The global average k_{zz} vs day of year for SABER at 96 km (dotted) and Qian et al. (2009). The mean k_{zz} for the compared plots is nearly identical, but there are significant differences in the intra-annual variations.

The Qian et al. determination of k_{zz} was deduced largely from satellite drag data, whereas the global average values are based on the O climatology in the MLT. At least one partial explanation is the intra-annual variation of [O] at 96 km (see Fig. 10), is similar but the intra-annual amplitude of [O] (and flux) is much less than the k_{zz} plot of Qian et al.

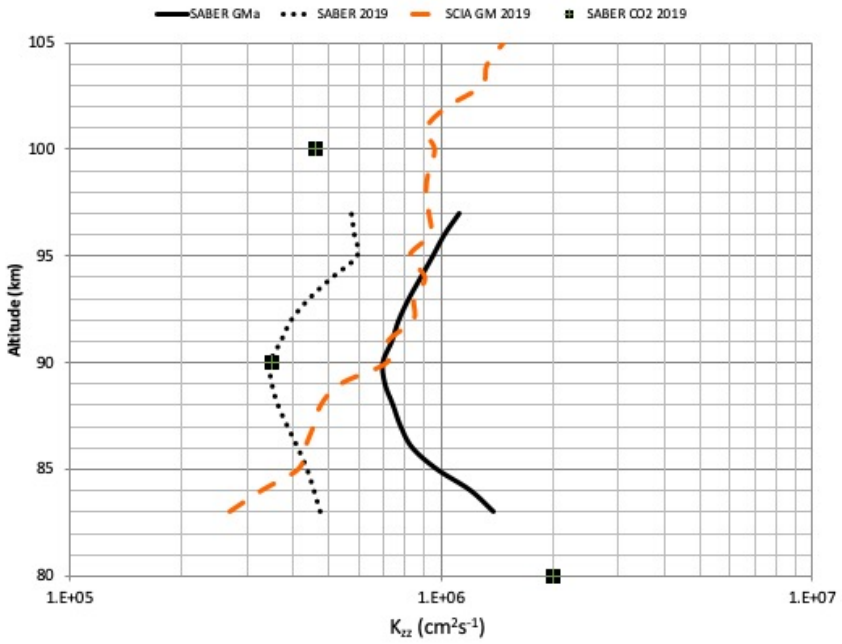

Fig 12. k_{zz} vs altitude for the global average (GA) of SABER O from this study are compared with the values determined in the S19 study.

An analysis of the factors responsible for the difference between the global mean k_{zz} from SABER in S19 and this study. One main cause is due to the [O] densities in this study being ~20% less at 96 km, and 50% lower at 83 km. The [O] column density, 80-96 km, is 33% less in this study, which results in a larger diffusion velocity. That is approximately 1/2 the difference. Other contributions are under study.

SUMMARY

The AO variation in k_{zz} peaks in summer (near solstice) and is a minimum in winter, with an amplitude change of a factor of 3-4x at 83 km between solstices. The AO amplitude of O density at 96 km determined herein (10%) and also by Chen et al. 2019 of 9.6% (and others) is consistent with the necessary change in flux between winter and summer. The climatology of the MLT k_{zz} supports the Qian et al. 2009 annual mean value, but not the variability in the downward flux at 96 km.

The analysis of k_{zz} in the EQ region revealed a large SAO amplitude of 3x from solstice to spring equinox, and 2x from summer solstice to fall equinox.

The annual-average EQ k_{zz} profiles are uniform with altitude, with a value of 1.1 10^6 cm^2s^{-1}. The uniformity with altitude and larger values than at mid latitudes are hypothesized to be due to;

1) the presence of the diurnal tide and subsequent turbulence from wave-tide coupling, and

2) less stratospheric wave filtering at the EQ allows waves generated in the troposphere to reach the MLT.

ACKNOWLEDGEMENTS AND REFERENCES

Acknowledgements: G. Swenson and F. Vargas are partially supported by NSF grants. We all extend our appreciation to the SABER team and the NASA for the continued operation and processing of SABER data which is essential for long term studies of MLT processes.

References

Colegrove, F. D., Hanson, W. B., & Johnson, F. S. (1965). Eddy diffusion and oxygen transport in the lower thermosphere. Journal of Geophysical Research, (1896-1977), 70 (19), 4931-4941.

Chen, Q., Kaufmann, M., Zhu, Y., Liu, J., Koppmann, R., & Riese, M. (2019). Global nighttime atomic oxygen abundances from GOMOS hydroxyl airglow measurements in the mesopause region. Atmospheric Chemistry and Physics,19 (22), 13891-13910.

Emmert, J. T., Drob, D. P., Picone, J. M., Siskind, D. E., Jones, M., Mlynczak, M. G., et al. (2020). NRLMSIS 2.0: A whole−atmosphere empirical model of temperature and neutral species densities. Earth and Space Science, 7, e2020EA001321, https://doi.org/10.1029/2020EA001321.

Lednyts'kyy, O., von Savigny, C., & Weber, M. (2017). Sensitivity of equatorial atomic oxygen in the MLT region to the 11-year and 27-day solar cycles. Journal of Atmospheric and Solar- Terrestrial Physics, 162 , 136 - 150.

Mlynczak, M. G., Hunt, L. A., Mast, J. C., Thomas Marshall, B., Russell, J. M.,Smith, A. K., . . . et al. (2013). Atomic oxygen in the mesosphere and lower thermosphere derived from SABER: Algorithm theoretical basis and measurement uncertainty. Journal of Geophysical Research: Atmospheres, 118 (11), 5724-5735.

Qian, L., Solomon, S. C., & Kane, T. J. (2009). Seasonal variation of thermospheric density and composition. Journal of Geophysical Research: Space Physics,114 (A1).

Swenson, G., Yee, Y., Vargas, F., & Liu, A. (2018). Vertical diffusion transport of atomic oxygen in the mesopause region consistent with chemical losses and continuity: Global mean and inter-annual variability. Journal of Atmospheric and Solar-Terrestrial Physics, 178 , 47-57.

Swenson, G. R., Salinas, C. C. J. H., Vargas, F., Zhu, Y., Kaufmann, M., Jones Jr., M., . . . Yee, J. H. (2019). Determination of global mean eddy diffusive transport in the mesosphere and lower thermosphere from atomic oxygen and carbon dioxide climatologies. Journal of Geophysical Research: Atmospheres,124 (23), 13519-13533.

Zhu, Y., Kaufmann, M., Ern, M., & Riese, M. (2015). Nighttime atomic oxygen in the mesopause region retrieved from SCIAMACHY O(1S) green line measurements and its response to solar cycle variation.Journal of Geophysical Research: Space Physics,120(10), 9057-9073.

ABSTRACT

The climatology of atomic oxygen in the MLT (mesosphere and lower thermosphere) is balanced by O production via photodissociation of O_2 in the lower thermosphere and recombination in the upper mesosphere. This work serves to establish a climatology of eddy diffusion and eddy diffusive velocity, including its intra-annual variations in the MLT based on the climatology of the region as a function of latitude and altitude. Atomic oxygen k_{zz} velocity profiles and fluxes (80-96 km) are balanced by the continuity of chemical loss, a method originally developed in the 1960's, was refined in 2019, in order to determine global mean k_{zz} profiles. In the current study, the intra-annual cycle was divided into twenty six (two-week periods) for each of three zones, the northern hemisphere (NH, 15 to 55^o), southern hemisphere (SH, -15 to -55^o), and the equatorial region (EQ, 15 to -15^o). Sixteen years of TIMED SABER O density measurements (2002-2018) and the most recent MSIS model N_2, O_2, H, and temperature profiles were used to calculate the chemical loss rates and determine the eddy diffusive velocities and fluxes of atomic oxygen. Our primary findings include a dominant SAO (semiannual oscillation) at all altitudes between 80-96 km at the equator, and a dominant AO (annual oscillation) below 87 km in the NH and SH, with a factor of 3-4 k_{zz} increase from winter to summer at 83 km. Although k_{zz} variability in the NH and SH is minimal at 96 km, an important height for thermospheric and ionospheric global circulation models, the O density increases by a factor of 1.5 between winter and summer.